This EarthArXiv pre-print is the revised version of a Matter Arising manuscript that has been under consideration by Nature. Given the significant time that required for peer-review process, we want to make the community aware of the problems in the original Nature paper (Ho et al. 2019). We will update the outcome of the review process.

Matters Arising

Unrealistic phytoplankton bloom trends in global lakes derived from Landsat measurements

Lian Feng[1,*], Yanhui Dai[1], Xuejiao Hou[2], Yang Xu[1], Junguo Liu[1], Chunmiao Zheng[1]

[1] School of Environmental Science and Engineering, Southern University of Science and Technology, Shenzhen, China. [2] State Key Laboratory of Information Engineering in Surveying, Mapping, and Remote Sensing, Wuhan University, Wuhan, China.
*Email: fengl@sustech.edu.cn

Given its advantages for synoptic and large-scale observations, satellite remote sensing has been widely used to effectively monitor the water quality of inland and coastal environments. Using satellite-derived reflectance data from the Landsat 5 Thematic Mapper (L5TM) as a proxy for algal bloom intensity, Ho et al. [1] showed an increase in peak summertime bloom intensity in 68% of the 71 large lakes worldwide from 1982 to 2012. However, we question the veracity of their finding for at least two reasons: (1) satellite-derived reflectance in a single near-infrared (NIR) band is not a reliable proxy for bloom strength due to the strong impacts of suspended sediments and aquatic vegetation, and (2) the infrequent satellite observations from L5TM (one cloud-free image every 1-2 months) make it difficult to draw statistically meaningful conclusions. Therefore, although it is natural to speculate that more blooms may be found in lakes under changing climatic conditions, the work by Ho et al. [1] needs to be revisited before reaching any solid conclusions.

Ho et al. [1] argued that the L5TM-estimated bloom intensity (B_{NIR}) (see Equation 2 in Ho et al. [1]), which is basically the reflectance in the NIR band, is correlated with chlorophyll-a (Chla) concentration or phytoplankton biomass. However, this argument became questionable when we examined the correlations between in situ Chla and water reflectance (in situ reflectance was aggregated into the NIR reflectance equivalent of band 4 of L5TM [2]) with data collected from 15 lakes in China and from waters with varying eutrophic status (Chla ranging between 1.5 and 222.6 mg m^{-3}) (see Extended Data Fig. 1). We revealed nonsignificant relationships ($p>0.05$) between near surface Chla and NIR reflectance in three different Chla ranges (full Chla range, Chla>50 mg m^{-3} and Chla>10 mg m^{-3}). Such complex relationships between spectral reflectance and Chla concentrations were also demonstrated by Spyrakos et al. [3] when using in situ data from various inland waters around the world. Theoretically, the signal in the NIR band can be attributed to various water constituents in addition to algal blooms, and the contributions from suspended sediments and the presence of aquatic plants could be two of the most common perturbations in inland lakes. Ho et al. [1] attempted to mask out waters associated with high sediment loads with the use of hue, but as detailed later, the hue defined in Ho et al. [1] does not accurately reflect the color of a water body and is thus not effective for distinguishing phytoplankton blooms from sediment-dominated waters.

Bloom strength tends to be substantially overestimated in sediment-rich waters. Examples from two of the lakes studied in Ho et al. [1] (Songkhla Lake in Thailand and Hongze Lake in China, see Fig. 1) show that the B_{NIR} of the high-turbidity, low-algae pixels (yellowish in true-color images) was higher than that of the algae-present pixels (greenish in true-color images) within the same images. The examination of true-color and the corresponding B_{NIR} images shows that historical L5TM observations have captured sediment plumes in at least 58 (82%) of the 71 studied lakes, and these plumes could be incorrectly labeled as algal blooms due to their high B_{NIR} values (see some examples in Extended Data Fig. 2). As well supported by previous studies using in situ data from both of the studied lakes in Ho et al. [1] and other global coastal/inland waters, the NIR reflectance in turbid waters can be substantially enhanced by sediment-induced strong backscattering signals (see Extended Data Table 1). In inland lakes, episodic meteorological (e.g., wind, precipitation) and hydrological (e.g., riverine discharge) events can strongly influence sediment concentrations [4], as exemplified by previous studies in Lake Erie[5] and Lake Okeechobee in the USA [6] and Hongze Lake in China [7] (three lakes examined in their study). As such, the impacts of water turbidity on B_{NIR} should be evaluated carefully.

Similar to high sediment loads, the growth of aquatic vegetation can lead to the overestimation of bloom severity. Pixels with high B_{NIR} values – in particular, vegetated waters (darkish in true-color images) rather than bloom areas – were also found within the same lakes (see Songkhla Lake in Fig. 1), where massive submerged plants have previously been reported [8]. The reason is that algal blooms and submerged vegetation share similar spectral curvatures and comparable magnitudes of NIR reflectance values, as demonstrated by the in situ hyperspectral measurements for Taihu Lake in China (a shallow lake that is ~200 km from Hongze Lake) (see Extended Data Fig. 3). Moreover, previous studies with datasets collected across various global regions and plant species also showed markedly increased NIR reflectance due to the presence of submerged vegetation (see Extended Data Table 2). Currently, challenges still exist when one attempts to distinguish submerged plants from algal blooms with multispectral satellite images, not to mention using a single NIR band [9]. Indeed, a literature search revealed that of the 71 studied lakes, 41 (58%) were found to contain abundant aquatic plants (see Extended Data Table 3), and their impacts on B_{NIR} should have been considered.

A hue-based mask (Equations 3 & 4 in Ho et al. [1]) was designed to exclude potential contamination from sediments. However, this approach has failed in numerous cases (see examples in Extended Data Fig. 2). This is mainly due to the inclusion of the atmospheric signals in the calculation of hue, i.e., the hue was estimated using the top-of-atmosphere (TOA) reflectance. Thus, this hue reflects the color of the combined signal of the atmosphere and the water, not the hue of the water itself. As shown in Extended Data Fig. 4, atmospheric molecular scattering (or Rayleigh scattering) alone could dominate the TOA reflectance for water bodies in the blue band [10]. Even worse, the method (i.e., Fmask [11]) used to determine lake surface area could lead to substantial underestimations of bloom severity. As the examples in Fig. 1c-e and Extended Data Fig. 5 show, when true-color images reveal in vivo bloom occurrences, such areas failed to pass the Fmask and were excluded in further B_{NIR} calculations. Indeed, the examination of their studied lakes showed that most of the severe blooms with surface scum were missed due to the improper use of Fmask. This is because intense blooms often cause high normalized difference vegetation index (NDVI) values that can exceed the threshold used by Fmask (e.g., $NDVI<0.1$) to identify water pixels [11]. Since the Fmask algorithm was originally designed for cloud and cloud-shadow detection [11], further considerations are required when it is used for water area identification.

Furthermore, the infrequent L5TM observations are well known for their limitations in terms of capturing the short- and long-term dynamics of lacustrine algal blooms. Such limitations could be exacerbated by frequent cloud distributions, which also pose one of the challenges associated with optical satellite remote sensing. Statistically, the global mean daily cloud-free probability is 33%, with seasonal differences of <5% [12]. In other words, when L5TM overpasses 23 times within a year because of its 16-day revisit period, the annual mean number of cloud-free observations for a given location is only ~7.5 even without any other unfavorable observational conditions (such as sun-glint). As a compromise between data availability and result fidelity, Ho et al [1] excluded those years with fewer than 3 valid images in five summer months. We replotted a time series of algal bloom areas in Taihu Lake that was produced by Hu et al. [13] (see Extended Data Fig. 6), which was obtained using cloud-free images from daily Moderate-resolution Imaging Spectroradiometer (MODIS) satellite observations (revisit period of ~1 image per day) between 2000 and 2008. Of the >300 cloud-free daily MODIS images within the 9-year period, only 24 shared the same overpassing dates as L5TM. Furthermore, detecting a bloom on the basis of remote sensing imagery depends strongly on wind, as the fraction of the satellite-observable surface bloom in relation to the total phytoplankton biomass is also a function of wind speed [14,15]. Due to the unpredictable nature of cloud occurrence and wind speed, the temporal dynamics of bloom features were difficult to characterize with L5TM datasets.

Our results have clearly demonstrated that the use of L5TM-based B_{NIR} by Ho et al. [1] as a proxy for algal bloom strength is questionable for the majority of the lakes examined in their study. The incorrect use of a water mask algorithm (i.e., Fmask) also leads to the omission of the most severe blooms with floating scum. The use of limited Landsat observations (often one cloud-free image every 1-2 months) is problematic for drawing statistically meaningful conclusions. Therefore, the trends in phytoplankton blooms for the 71 global lakes derived by Ho et al. [1] appear unrealistic. In summary, a significant amount of work, including the development of reliable algorithms for bloom detection and the use of statistically meaningful observations, is still required to estimate the multidecadal changes in bloom conditions before any attempt is made to interpret such "changes."

Data availability The Landsat data can be obtained from the U.S. Geological Survey at https://glovis.usg.gov. The in situ spectral and Chla data will be provided to the public upon acceptation of this manuscript.

References

1 Ho, J., Michalak, A. & Pahlevan, N. Widespread global increase in intense lake phytoplankton blooms since the 1980s. *Nature*, 1-1 (2019).

2 Kalman, L. S. & Peltzer, G. R. Simulation of Landsat Thematic Mapper imagery using AVIRIS hyperspectral imagery. (1993).

3 Spyrakos, E. *et al.* Optical types of inland and coastal waters. *Limnology and Oceanography* **63**, 846-870, doi:10.1002/lno.10674 (2018).

4 Bloesch, J. Mechanisms, measurement and importance of sediment resuspension in lakes. *Marine and Freshwater Research* **46**, 295-304 (1995).

5 Valipour, R., Boegman, L., Bouffard, D. & Rao, Y. R. Sediment resuspension mechanisms and their contributions to high-turbidity events in a large lake. *Limnology and Oceanography* **62**, 1045-1065, doi:10.1002/lno.10485 (2017).

6 Wang, M., Nim, C. J., Son, S. & Shi, W. Characterization of turbidity in Florida's Lake Okeechobee and Caloosahatchee and St. Lucie estuaries using MODIS-Aqua measurements. *Water research* **46**, 5410-5422 (2012).

7 Cao, Z., Duan, H., Feng, L., Ma, R. & Xue, K. Climate-and human-induced changes in suspended particulate matter over Lake Hongze on short and long timescales. *Remote sensing of environment* **192**, 98-113 (2017).

8 Sompongchaiyakul, P., Laongsiriwong, N. & Sangkarnjanawanich, P. An occurrence of eutrophication in Songkhla Lake: A review. *Proceedings of the International Workshop on Integrated Lake Management, Hai-Yai, Songkhla*, 19-21 (2004).

9 Luo, J. *et al.* Mapping species of submerged aquatic vegetation with multi-seasonal satellite images and considering life history information. *International Journal of Applied Earth Observation and Geoinformation* **57**, 154-165 (2017).

10 Gordon, H. R. Atmospheric correction of ocean color imagery in the Earth Observing System era. *J. Geophys. Res.* **102**, 17081-17106 (1997).

11 Zhu, Z., Wang, S. & Woodcock, C. E. Improvement and expansion of the Fmask algorithm: Cloud, cloud shadow, and snow detection for Landsats 4–7, 8, and Sentinel 2 images. *Remote Sensing of Environment* **159**, 269-277 (2015).

12 King, M. D., Platnick, S., Menzel, W. P., Ackerman, S. A. & Hubanks, P. A. Spatial and temporal distribution of clouds observed by MODIS onboard the Terra and Aqua satellites. *IEEE Transactions on Geoscience and remote sensing* **51**, 3826-3852 (2013).

13 Hu, C. *et al.* Moderate resolution imaging spectroradiometer (MODIS) observations of cyanobacteria blooms in Taihu Lake, China. *Journal of Geophysical Research: Oceans* **115** (2010).

14 Qi, L., Hu, C., Visser, P. M. & Ma, R. Diurnal changes of cyanobacteria blooms in Taihu Lake as

derived from GOCI observations. *Limnology and Oceanography* **63**, 1711-1726 (2018).

15 Bosse, K. R. *et al.* Spatial-temporal variability of in situ cyanobacteria vertical structure in Western Lake Erie: Implications for remote sensing observations. *Journal of Great Lakes Research* **45**, 480-489, doi:https://doi.org/10.1016/j.jglr.2019.02.003 (2019).

Author contributions L.F. initiated the project and wrote an initial draft of the manuscript, and Y.D., X.H., and Y.X. performed the data processing and analysis. All authors participated in interpreting the results and revising the manuscript.

Competing interests Declared none.

Additional information

Supplementary information accompanies this Comment.

Correspondence and requests for materials should be addressed to L.F.

Acknowledgements This work was supported by the Strategic Priority Research Program of Chinese Academy of Sciences (XDA20060402) and the National Natural Science Foundation of China (41971304, 41671338, 41890852 and 41890851).

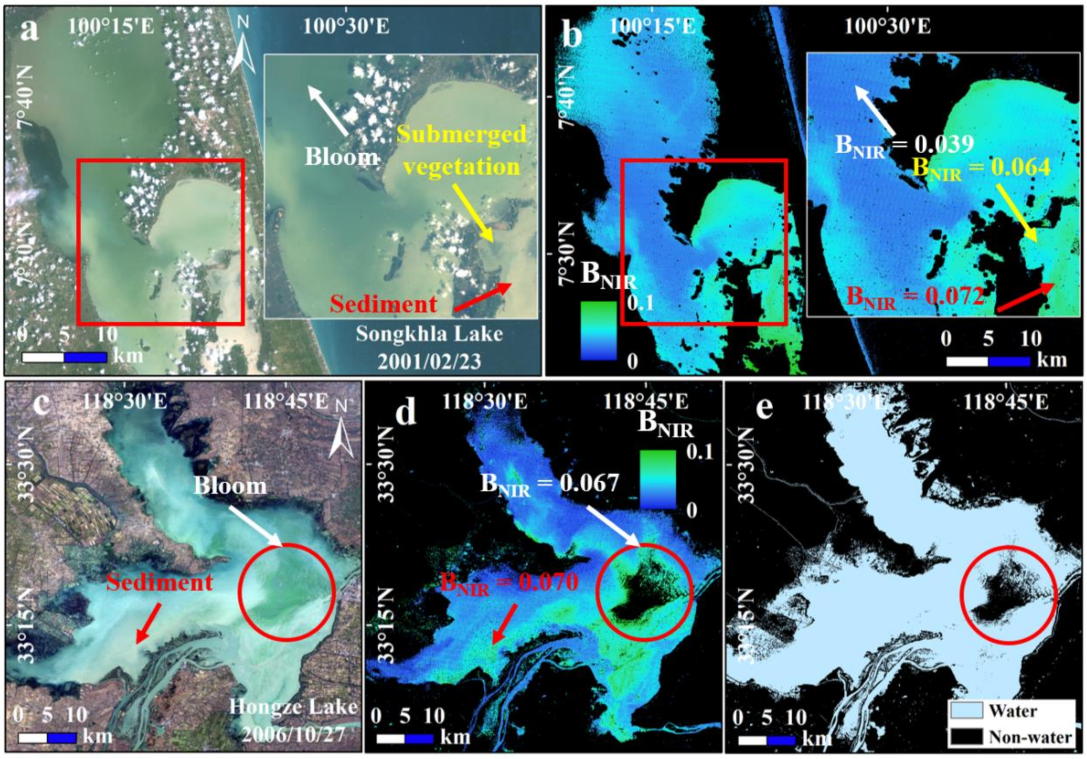

Figure 1 | Examples showing the problems associated with L5TM-based bloom intensity (B_{NIR}, estimated with Equation 2 in Ho et al. [1]) in global lacustrine phytoplankton bloom detection. L5TM true-color composites and corresponding B_{NIR} map for Songkhla Lake in Thailand (**a-b**) and Hongze Lake in China (**c-d**). (**e**) Water mask determined by Fmask[11] for Hongze Lake using the same image in **c**. Areas with either high sediment loads (yellowish in true-color images, indicated by red arrows) or the presence of submerged vegetation (darkish in true-color images, indicated by yellow arrows) exhibit higher B_{NIR} values than the bloom-occurring pixels (greenish in true-color images, indicated by white arrows), leading to erroneous interpretation of algal blooms. An intense bloom in Hongze Lake (within the red circle) has been erroneously classified as non-water by Fmask and excluded in the B_{NIR} map (**d**). More examples of these problems in many other lakes studied in Ho et al [1] are available in the Extended Data Figs. 2&5. The red squares within panels a & b indicate inset location.

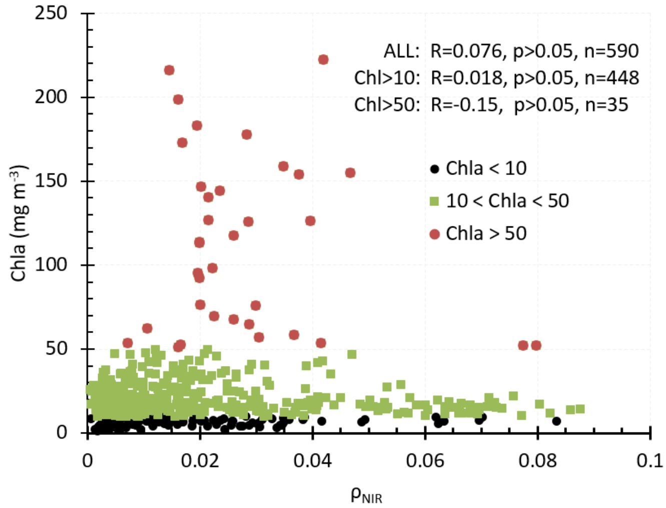

Extended Data Figure 1 | Relationship between Chla and the surface reflectance in the NIR band (ρ_{NIR}). The correlations for different Chla ranges are examined.The data are from in situ measurements collected in 15 lakes in China across waters with varying eutrophic status. ρ_{NIR} values are the equivalent L5TM NIR reflectances aggregated using in situ hyperspectral measurements and the L5TM spectral response function (see the aggregation method in Kalmen et al. [2]).

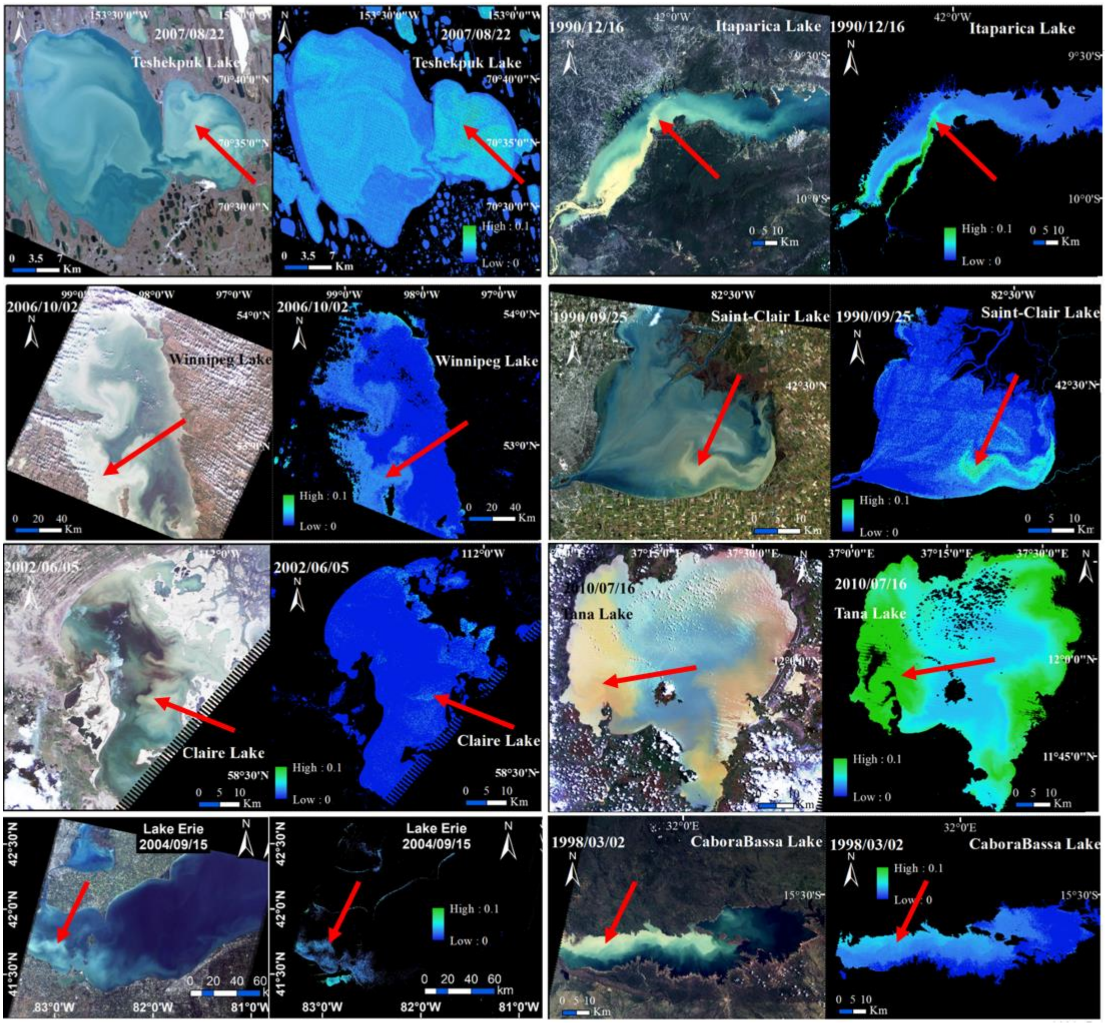

Extended Data Figure 2 | Examples showing the impacts of high sediment loads on the bloom intensity (B_{NIR}) calculations in eight of the studied lakes in Ho et al. [1]. The left panels of the paired images show the true-color composites for L5TM images, and the right panels show the corresponding B_{NIR} maps after applying the hue and Fmask masks. The sediment plumes (indicated by red arrows), with high B_{NIR} values (~0.1), could still be classified as intense blooms with the hue mask defined in Ho et al. [1]. The examination of historical L5TM images show that sediment plumes could occur in at least 58 (81.7%) of the 71 lakes studied in Ho et al. [1].

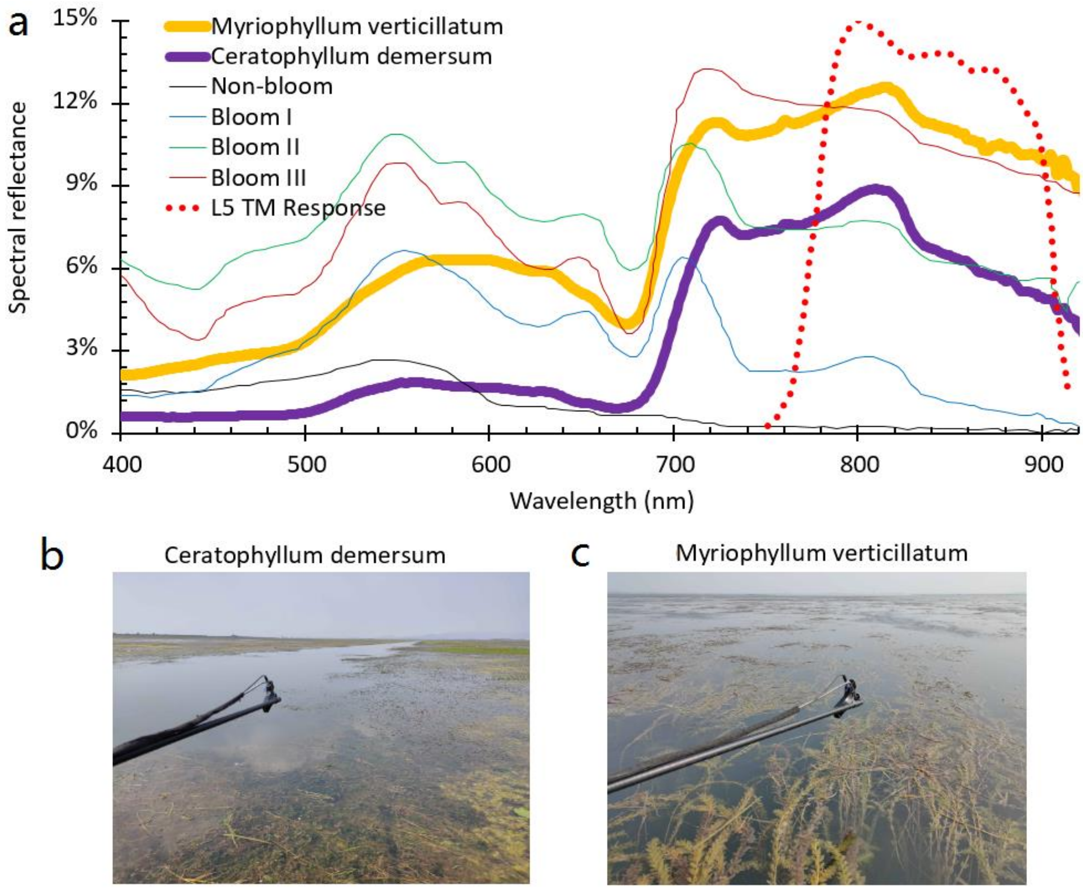

Extended Data Figure 3 | Reflectance spectra of submerged vegetation. (**a**) The spectral reflectances of two types (*Ceratophyllum demersum* and *Myriophyllum verticillatum*) of submerged vegetation collected in Taihu Lake in China on October 24, 2019, with the PSR+3500 field-portable spectrometer manufactured by Spectral Evolution. Also plotted are the spectral reflectances of different blooms and the normalized spectral responses in the L5TM NIR band, which were obtained from Extended Data Fig. 7 in Ho et al. [1]. The spectral features of submerged vegetation, particularly the reflectance in the NIR band, are very similar to those of intense phytoplankton blooms. (**b**) and (**c**) show photos taken while conducting the in situ measurements.

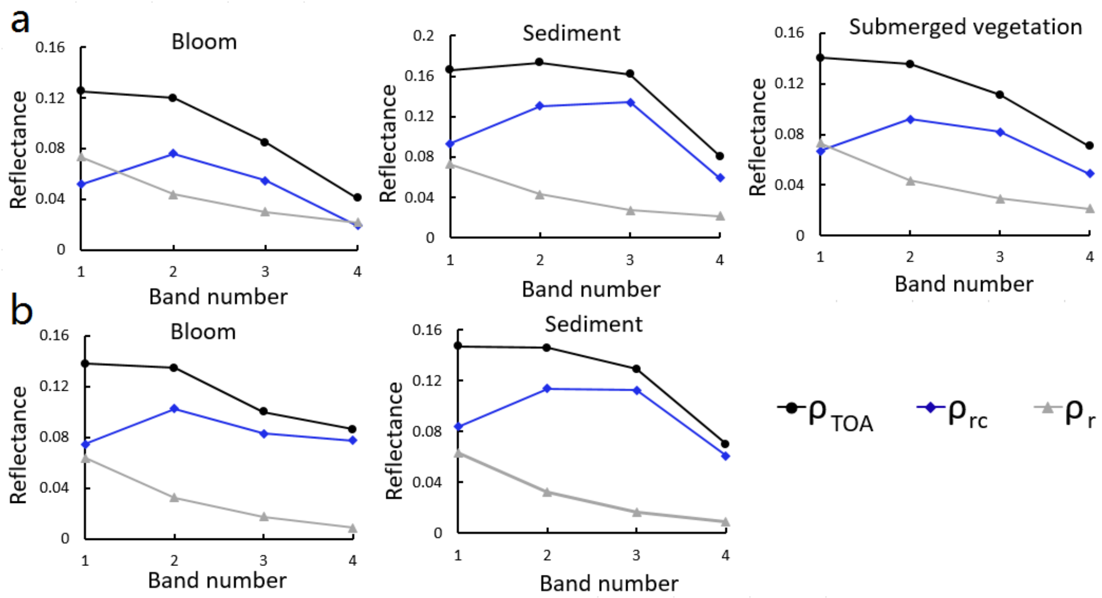

Extended Data Figure 4 | Spectral features of different types of waters in L5TM images. The spectral data were obtained from the arrow-indicated pixels in Fig. 1 ((**a**) from Songkhla Lake and (**b**) from Hongze Lake). ρ_{TOA} is the top-of-atmosphere reflectance, ρ_r is the reflectance from Rayleigh scattering (estimated using the method in Gordon [10]) and ρ_{rc} is the difference between ρ_{TOA} and ρ_r.

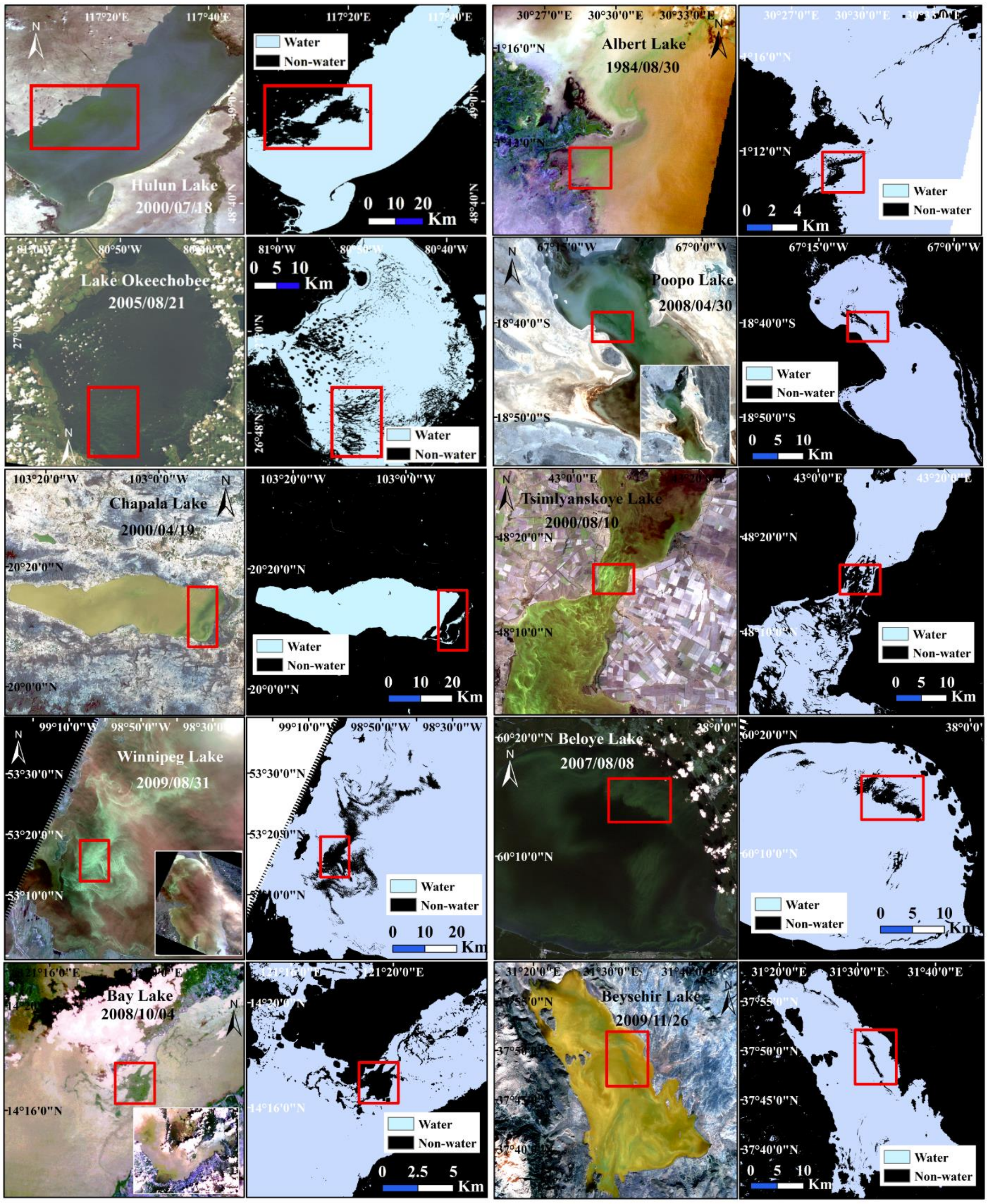

Extended Data Figure 5 | Examples showing the pixels with intense blooms erroneously masked by Fmask in ten of the studied lakes in Ho et al. [1]. The left panels of the paired images show the true-color composites for the L5TM images, and the right panels show the resultant separation of pixels determined using Fmask. Clearly, intense blooms (greenish in the red squares) have been classified as other classes rather than as water. The examination of their studied lakes showed that most of the severe blooms with surface scum were missed due to the improper use of Fmask.

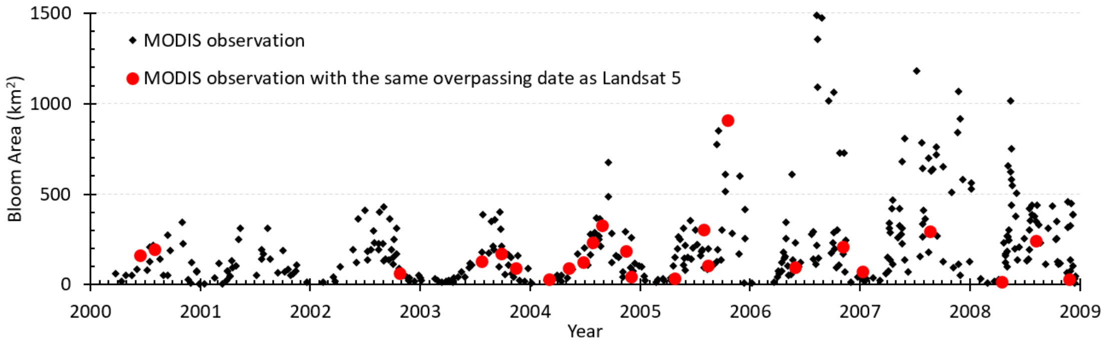

Extended Data Figure 6 | Daily areas of algal bloom in Taihu Lake between 2000 and 2008 determined using MODIS observations by Hu et al.[13]. Red points represent MODIS observations with the same overpassing dates as L5TM (i.e., daily MODIS observations have concurrent L5TM images), and indicate the difficulty in characterizing long-term bloom dynamics. For example, while black dots show a clear increase in bloom area after 2005, such a trend is difficult to capture with the red dots.

Extended Data Table 1 | A list of previous studies wherein in situ datasets showed substantial impacts of water turbidity (or total suspended sediments, TSS) on the reflectance of the water column at NIR band. The bolded text indicates studies of lakes that were also included in Ho et al. [1] Note that this table does not include all related studies, since a complete list would be too long to present here.

References	Location(s)	Range of turbidity (NTU) /TSS (mg/L)
Büttner et al. [16]	**Balaton Lake, Hungary**	**69.0-591.0 mg/L**
Bukata et al. [17]	**Saint-Clair Lake, Canada and United States**	**2.5-20.0 mg/L**
Nas et al. [18]	**Beysehir Lake, Turkey**	**0.1-15.5 mg/L**
Binding et al. [19]	**Lake Erie, United States**	**0.18-28.26 mg/L**
Matthews et al. [20]	**Zeekoevlei Lake, South Africa**	**0.03-50 mg/L**
Wang et al. [6]	**Lake Okeechobee, United States**	**1-300 NTU**
Kaba et al. [21]	**Tana Lake, Ethiopia**	**~0-240.0 mg/L**
Hamed [22]	**Nasser Lake, Egypt**	**0.75-78.4 NTU**
Zeng & Binding [23]	**Winnipeg Lake, Canada, and Lake Erie, Canada and United States**	**0.01-31.6 mg/L**
Mikkelsen [24]	Four coastal regions, Denmark and Ebro River, Spain	0.5-24.6 mg/L
Dekker et al. [25]	Frisian lakes, Netherlands	1.6-255.0 mg/L
Doxaran et al [26]	Gironde Estuary, France	35-2072 mg/L
Koponen et al [27]	Four lakes in Finland	0-30 NTU
Liu et al. [28]	Middle Yangtze River, China	23.4–61.2 mg/L
Sterckx et al. [29]	Scheldt River, Belgium	13-336 mg/L
Oyama et al. [30]	Lake Kasumigaura, Japan	17.6-47.9 mg/L
Tarrant et al. [31]	Roosevelt and Bartlett Pleasant Lake, United States	0.30–13.4 mg/L
Nechad et al. [32]	Southern North Sea, Europe	1.24-110.27 mg/L
Chen et al. [33]	Apalachicola Bay, United States	1.29–208 mg/L
Knaeps et al. [34]	Scheldt, Belgium and the Netherlands	15-402 mg/L
Long & Pavelsky [35]	Peace–Athabasca Delta, Canada	0-4000 mg/L
Giardino et al. [36]	Lake Maggiore, Italy	0.5-100 mg/L
Feng et al. [37]	Yangtze Estuary, China	4.3-1762.1 mg/L
Dorji & Fearns [38]	Simulated datasets	0.01-7000.0 mg/L
Dogliotti et al. [39]	Southern North Sea; Guyana coastal waters, Scheldt, Gironde, France; and Río de la Plata estuary, South America	1.8-988 mg/L
Han et al. [40]	European coastal waters; French Guiana; Eastern Vietnam Sea; China Yellow Sea; and northern Canada	0.15-2626.0 mg/L
Yu et al. [41]	Gulf of Mexico and Massachusetts Bay, United States; Yangtze Estuary, China; European coastal waters; the Río de La Plata Estuary, South America	0.2-2068.8 mg/L

Extended Data Table 2 | A list of previous studies wherein in situ datasets showed that NIR reflectance could be substantially enhanced due to the presence of submerged vegetation. Note that this table does not include all related studies, since a complete list would be too long to present here.

References	Location(s)	Major vegetation species
Zhang et al. [42]	Honghu Lake, China	*Potamogeton maackianus* Benn., *Myriophyllum spicatum, Hydrilla verticillata* Royle, *Ceratophyllum oryzetorum* Kom. *and Potamogeton lucens* Linn.
Vahtmäe et al. [43]	Baltic Sea, Europe	*Cladophora glomerata, Furcellaria lumbricalis, and Fucus vesiculosus*
Dogan et al. [44]	Lake Mogan,Turkey	*Potamogeton pectinatus, Najas sp and Myriophyllum spicatum*
Yuan & Zhang [45]	Chongming Island, China	*Myriophyllum spicatum*
Yadav et al. [46]	Lake Biwa, Japan	Unknown
Pu et al. [47]	Florida coast, United States	*Syringodium filiforme, Thalassia testudinum,and Halodule wrightii.*
Visser et al. [48]	River Wylye and River Frome, UK	*Myriophyllum spicatum, Ranunculus fluitans and Potamogeton pectinatus*
Watanabe et al. [49]	Ferreira stream, Brazil	*Ceratophyllum demersum*
Giardino et al. [50]	Lake Trasimeno, Italy	*Potamogeton pectinatusand Myriophyllum spicatum*
Oyama et al. [51]	Lakes Kasumigaura, Inba-numa and Tega-numa, Japan	*Trapa natans*
Santos et al. [52]	Sacramento San Joaquin River Delta, United States	*Myriophyllum spicatum and Egeria densa*
Luo et al. [53]	Lake Taihu, China	*Vallisneria spiralis, Ceratophyllum demersum, Potamogeton malaianus, P. maackianus,* and *Hydrilla verticillata*
Hou et al. [54]	25 lakes, China	Unknown
Brooks et al. [55]	Lake Huron, United States	*M. spicatum and Myriophyllum sibiricum*
Fritz et al. [56]	Lake Starnberg, Germany	*Chara spp.and Potamogeton spp.*
Ghirardi et al. [57]	Lake Iseo, Italy	*Vallisneria spiralis and Najas marina*
Niroumand-Jadidi [58]	Sarca River, Italy	Unknown
Wilson et al. [59]	Atlantic coast of Nova Scotia, Canada	*Zostera marina*

Extended Data Table 3 | List of studied lakes in Ho et al.[1] with abundant submerged vegetation identified.

ID	Lake name	Country	References
1	Clear	United States	Niemeier and Hubert [60]
2	Claire	Canada	Toshner and Region-Brule [61]
3	Simcoe	Canada	Depew et al. [62]
4	Bay	Philippines	Vicencio and Buot Jr [63]
5	CaboraBassa	Mozambique Zimbabwe	Bond and Roberts [64]
6	Balaton	Hungary	Istvánovics et al. [65]
7	Saint-Clair	Canada United States	French III [66]
8	Dauphin	Canada	Balesic [67]
9	Khanka	Russia China	Li et al. [68]
10	Hongze	China	Liu et al. [69]; Shengzhao [70]
11	Alexandrina	Australia	Ward and Talbot [71]
12	Bosten	China	Wang and Dou [72]
13	Okeechobee	United States	Havens et al. [73]
14	Poopo	Bolivia	García et al. [74]
15	Hulun	China	Fang et al. [75]
16	Songkhla	Thailand	Sompongchaiyakul et al. [8]
17	Qinghai	China	Chen [76]
18	Gyaring	China	Pen [77]
19	Ulungar	China	Li [78]
20	Ngoring	China	Pen [77]
21	Se-lin	China	Wang and Dou [72]
22	Kariba	Zimbabwe Zambia	Machena [79]
23	Aral-Sea	Kazakhstan Uzbekistan	Aladin et al. [80]
24	Winnebago	United States	Gabriel and Bodensteiner [81]
25	Erie	Canada United States	Badzinski et al. [82]
26	Baikal	Russia	Chepinoga et al. [83]
27	Chilka	India	Jaikumar et al. [84]
28	Cha-jihNan-mu-tso--Zhari-Namco	China	Wang and Dou [72]
29	Beloye	Russia	Krivonogov et al. [85]
30	Sasykkol	Kazakhstan	Romanova and Kazangapova [86]
31	Chapala	Mexico	Villamagna et al. [87]
32	Balkhash	Kazakhstan	Imentai et al. [88]
33	Izabal	Guatemala	Barrientos [89]
34	Urmia	Iran	Tehranchi et al. [90]
35	Nicaragua	Nicaragua	Davies [91]
36	Alakol	Kazakhstan	Romanova and Kazangapova [86]
37	Victoria	Tanzania Uganda Kenya	Cheruiyot et al. [92]
38	Sevan	Armenia	Heblinski et al. [93]
39	Beysehir	Turkey	Beklioglu et al. [94]
40	Nasser	Egypt Sudan	Green [95]
41	Edward	Zaire Uganda	Green [96]

References

16 Büttner, G., Korándi, M., Gyömörei, A., Köte, Z. & Szabó, G. Satellite remote sensing of inland waters: Lake Balaton and reservoir Kisköre. *Acta Astronautica* **15**, 305-311 (1987).

17 Bukata, R., Jerome, J. & Bruton, J. Particulate concentrations in Lake St. Clair as recorded by a shipborne multispectral optical monitoring system. *Remote Sensing of Environment* **25**, 201-229 (1988).

18 Nas, B., Ekercin, S., Karabörk, H., Berktay, A. & Mulla, D. An application of Landsat-5TM image data for water quality mapping in Lake Beysehir, Turkey. *Water, Air, Soil Pollution* **212**, 183-197 (2010).

19 Binding, C., Jerome, J., Bukata, R. & Booty, W. Suspended particulate matter in Lake Erie derived from MODIS aquatic colour imagery. *International Journal of Remote Sensing* **31**, 5239-5255 (2010).

20 Matthews, M. W., Bernard, S. & Winter, K. Remote sensing of cyanobacteria-dominant algal blooms and water quality parameters in Zeekoevlei, a small hypertrophic lake, using MERIS. *Remote Sensing of Environment* **114**, 2070-2087 (2010).

21 Kaba, E., Philpot, W. & Steenhuis, T. Evaluating suitability of MODIS-Terra images for reproducing historic sediment concentrations in water bodies: Lake Tana, Ethiopia. *International Journal of Applied Earth Observation* **26**, 286-297 (2014).

22 Hamed, M. A. Estimation of water quality parameters in Lake Nasser using remote sensing techniques. (2017).

23 Zeng, C. & Binding, C. The Effect of Mineral Sediments on Satellite Chlorophyll-a Retrievals from Line-Height Algorithms Using Red and Near-Infrared Bands. *Remote Sensing* **11**, 2306 (2019).

24 Mikkelsen, O. A. Variation in the projected surface area of suspended particles: Implications for remote sensing assessment of TSM. *Remote Sensing of Environment* **79**, 23-29 (2002).

25 Dekker, A., Vos, R. & Peters, S. Comparison of remote sensing data, model results and in situ data for total suspended matter (TSM) in the southern Frisian lakes. *Science of the Total Environment* **268**, 197-214 (2001).

26 Doxaran, D., Froidefond, J.-M., Lavender, S. & Castaing, P. Spectral signature of highly turbid waters: Application with SPOT data to quantify suspended particulate matter concentrations. *Remote sensing of Environment* **81**, 149-161 (2002).

27 Koponen, S., Pulliainen, J., Kallio, K. & Hallikainen, M. Lake water quality classification with airborne hyperspectral spectrometer and simulated MERIS data. *Remote Sensing of Environment* **79**, 51-59 (2002).

28 Liu, J. P. *et al.* Sedimentary features of the Yangtze River-derived along-shelf clinoform deposit in the East China Sea. *Continental Shelf Research* **26**, 2141-2156 (2006).

29 Sterckx, S., Knaeps, E., Bollen, M., Trouw, K. & Houthuys, R. Retrieval of suspended sediment from advanced hyperspectral sensor data in the Scheldt estuary at different stages in the tidal cycle. *Marine Geodesy* **30**, 97-108 (2007).

30 Oyama, Y., Matsushita, B., Fukushima, T., Matsushige, K. & Imai, A. Application of spectral decomposition algorithm for mapping water quality in a turbid lake (Lake Kasumigaura, Japan) from Landsat TM data. *ISPRS Journal of Photogrammetry Remote sensing* **64**, 73-85 (2009).

31 Tarrant, P., Amacher, J. & Neuer, S. Assessing the potential of Medium‐Resolution Imaging Spectrometer (MERIS) and Moderate‐Resolution Imaging Spectroradiometer (MODIS) data

for monitoring total suspended matter in small and intermediate sized lakes and reservoirs. *Water Resources Research* **46** (2010).

32 Nechad, B., Ruddick, K. & Park, Y. Calibration and validation of a generic multisensor algorithm for mapping of total suspended matter in turbid waters. *Remote Sensing of Environment* **114**, 854-866 (2010).

33 Chen, S., Huang, W., Chen, W. & Chen, X. An enhanced MODIS remote sensing model for detecting rainfall effects on sediment plume in the coastal waters of Apalachicola Bay. *Marine environmental research* **72**, 265-272 (2011).

34 Knaeps, E., Dogliotti, A. I., Raymaekers, D., Ruddick, K. & Sterckx, S. In situ evidence of non-zero reflectance in the OLCI 1020 nm band for a turbid estuary. *Remote Sensing of Environment* **120**, 133-144 (2012).

35 Long, C. M. & Pavelsky, T. M. Remote sensing of suspended sediment concentration and hydrologic connectivity in a complex wetland environment. *Remote Sensing of Environment* **129**, 197-209 (2013).

36 Giardino, C., Bresciani, M., Stroppiana, D., Oggioni, A. & Morabito, G. Optical remote sensing of lakes: an overview on Lake Maggiore. *J. Limnol* **73**, 201-214 (2014).

37 Feng, L., Hu, C., Chen, X. & Song, Q. Influence of the Three Gorges Dam on total suspended matters in the Yangtze Estuary and its adjacent coastal waters: Observations from MODIS. *Remote Sensing of Environment* **140**, 779-788 (2014).

38 Dorji, P. & Fearns, P. A quantitative comparison of total suspended sediment algorithms: A case study of the last decade for MODIS and landsat-based sensors. *Remote Sensing* **8**, 810 (2016).

39 Dogliotti, A. I., Ruddick, K., Nechad, B., Doxaran, D. & Knaeps, E. A single algorithm to retrieve turbidity from remotely-sensed data in all coastal and estuarine waters. *Remote Sensing of Environment* **156**, 157-168 (2015).

40 Han, B. *et al.* Development of a semi-analytical algorithm for the retrieval of suspended particulate matter from remote sensing over clear to very turbid waters. *Remote Sensing* **8**, 211 (2016).

41 Yu, X. *et al.* An empirical algorithm to seamlessly retrieve the concentration of suspended particulate matter from water color across ocean to turbid river mouths. *Remote Sensing of Environment* **235**, 111491 (2019).

42 Zhang, X. On the estimation of biomass of submerged vegetation using Landsat thematic mapper (TM) imagery: a case study of the Honghu Lake, PR China. *International Journal of Remote Sensing* **19**, 11-20 (1998).

43 Vahtmäe, E., Kutser, T., Martin, G. & Kotta, J. Feasibility of hyperspectral remote sensing for mapping benthic macroalgal cover in turbid coastal waters—a Baltic Sea case study. *Remote Sensing of Environment* **101**, 342-351 (2006).

44 Dogan, O. K., Akyurek, Z. & Beklioglu, M. Identification and mapping of submerged plants in a shallow lake using quickbird satellite data. *Journal of environmental management* **90**, 2138-2143 (2009).

45 Yuan, L. & Zhang, L.-Q. Mapping large-scale distribution of submerged aquatic vegetation coverage using remote sensing. *Ecological Informatics* **3**, 245-251 (2008).

46 Yadav, S. *et al.* A satellite-based assessment of the distribution and biomass of submerged aquatic vegetation in the optically shallow basin of Lake Biwa. *Remote Sensing* **9**, 966 (2017).

47 Pu, R., Bell, S., Baggett, L., Meyer, C. & Zhao, Y. Discrimination of seagrass species and cover

classes with in situ hyperspectral data. *Journal of Coastal Research* **28**, 1330-1344 (2012).

48 Visser, F., Wallis, C. & Sinnott, A. M. Optical remote sensing of submerged aquatic vegetation: Opportunities for shallow clearwater streams. *Limnologica* **43**, 388-398 (2013).

49 Watanabe, F. S. Y., Imai, N. N., Alcântara, E. H., da Silva Rotta, L. H. & Utsumi, A. G. Signal Classification of Submerged Aquatic Vegetation Based on the Hemispherical–Conical Reflectance Factor Spectrum Shape in the Yellow and Red Regions. *Remote Sensing* **5**, 1856-1874 (2013).

50 Giardino, C. *et al.* Airborne hyperspectral data to assess suspended particulate matter and aquatic vegetation in a shallow and turbid lake. *Remote Sensing of Environment* **157**, 48-57 (2015).

51 Oyama, Y., Matsushita, B. & Fukushima, T. Distinguishing surface cyanobacterial blooms and aquatic macrophytes using Landsat/TM and ETM+ shortwave infrared bands. *Remote Sensing of Environment* **157**, 35-47, doi:https://doi.org/10.1016/j.rse.2014.04.031 (2015).

52 Santos, M. J., Anderson, L. W. & Ustin, S. L. Effects of invasive species on plant communities: an example using submersed aquatic plants at the regional scale. *Biological Invasions* **13**, 443-457 (2011).

53 Luo, J. *et al.* Applying remote sensing techniques to monitoring seasonal and interannual changes of aquatic vegetation in Taihu Lake, China. *Ecological Indicators* **60**, 503-513 (2016).

54 Hou, X., Feng, L., Chen, X. & Zhang, Y. Dynamics of the wetland vegetation in large lakes of the Yangtze Plain in response to both fertilizer consumption and climatic changes. *ISPRS Journal of Photogrammetry Remote Sensing* **141**, 148-160 (2018).

55 Brooks, C. N., Grimm, A. G., Marcarelli, A. M. & Dobson, R. J. Multiscale collection and analysis of submerged aquatic vegetation spectral profiles for Eurasian watermilfoil detection. *Journal of Applied Remote Sensing* **13**, 037501 (2019).

56 Fritz, C., Kuhwald, K., Schneider, T., Geist, J. & Oppelt, N. Sentinel-2 for mapping the spatio-temporal development of submerged aquatic vegetation at Lake Starnberg (Germany). *Journal of Limnology* **78** (2019).

57 Ghirardi, N. *et al.* Spatiotemporal Dynamics of Submerged Aquatic Vegetation in a Deep Lake from Sentinel-2 Data. *Water* **11**, 563 (2019).

58 Niroumand-Jadidi, M., Pahlevan, N. & Vitti, A. Mapping substrate types and compositions in shallow streams. *Remote Sensing* **11**, 262 (2019).

59 Wilson, K. L., Skinner, M. A. & Lotze, H. K. Eelgrass (Zostera marina) and benthic habitat mapping in Atlantic Canada using high-resolution SPOT 6/7 satellite imagery. *Estuarine, Coastal Shelf Science* **226**, 106292 (2019).

60 Niemeier, P. E. & Hubert, W. A. The 85-year history of the aquatic macrophyte species composition in a eutrophic prairie lake (United States). *Aquatic Botany* **25**, 83-89 (1986).

61 Toshner, S. & Region-Brule, N. Fishery Survey–Middle Eau Claire Lake Bayfield County, 2004-2005 WBIC Code–2742100. (2006).

62 Depew, D. C., Houben, A. J., Ozersky, T., Hecky, R. E. & Guildford, S. J. Submerged aquatic vegetation in Cook's Bay, Lake Simcoe: assessment of changes in response to increased water transparency. *Journal of Great Lakes Research* **37**, 72-82 (2011).

63 Vicencio, E. J. M. & Buot Jr, I. E. Aquatic weed flora on the Southwest Lakeside of Laguna De Bay. *J Wetl Biodivers* **7**, 75-90 (2017).

64 Bond, W. & Roberts, M. The colonization of Cabora Bassa, Moçambique, a new man-made lake,

by floating aquatic macrophytes. *Hydrobiologia* **60**, 243-259 (1978).
65 Istvánovics, V., Honti, M., Kovács, Á. & Osztoics, A. Distribution of submerged macrophytes along environmental gradients in large, shallow Lake Balaton (Hungary). *Aquatic Botany* **88**, 317-330 (2008).
66 French III, J. R. Effect of submersed aquatic macrophytes on resource partitioning in yearling rock bass (Ambloplites rupestris) and pumpkinseeds (Lepomis gibbosus) in Lake St. Clair. *Journal of Great Lakes Research* **14**, 291-300 (1988).
67 Balesic, H. Comparative ecology of four species of darters (Etheostominae) in Lake Dauphin and its tributary, the Valley River. (1971).
68 Li, R., Zhang, Q.-Z., Jiang, Y.-B., Zhang, L. & Shao, X.-M. Species Diversity of Plant Communities of Xingkai Lake Wetlands under Different Levels of Disturbance. *Wetland Science* **9**, 179-184 (2011).
69 Liu, W., Deng, W., Wang, G., Li, A. & Zhou, J. Aquatic macrophyte status and variation characteristics in the past 50 years in Hongzehu Lake. *J. Hydroecol* **2**, 1-8 (2009).
70 Shengzhao, Z. Aquatic vegetation in Hongze Lake. *Journal of Lake Sciences* **1** (1992).
71 Ward, J. & Talbot, J. Distribution of aquatic macrophytes in Lake Alexandrina, New Zealand. *New Zealand journal of marine and freshwater research* **18**, 211-220 (1984).
72 Wang, S. & Dou, H. *Chinese Lake Cataloges*. (Science Press, 1998).
73 Havens, K. E., Fox, D., Gornak, S. & Hanlon, C. Aquatic vegetation and largemouth bass population responses to water-level variations in Lake Okeechobee, Florida (USA). *Hydrobiologia* **539**, 225-237 (2005).
74 García, M. *et al.* Heavy metals in aquatic plants and their relationship to concentrations in surface water, groundwater and sediments-A case study of Poopó basin, Bolivia. *Revista Boliviana de Química* **22**, 11-18 (2005).
75 Fang, C. *et al.* Remote sensing of harmful algal blooms variability for Lake Hulun using adjusted FAI (AFAI) algorithm. *J. Environ. Inf. http://dx. doi. org/10.3808/jei* **201700385** (2018).
76 Chen, Y. Studies on the potamogetonaceae in Qinghai Lake. *Acta Hydrobiol Sin* **11**, 228-235 (1987).
77 Pen, M. Vegetation types and distributions around Gyaring Lake and Ngoring Lake. *Acta Biological Plateau Sinica* **7**, 71-79 (1987).
78 Li, W. Study on aquatic vegetation in Wulungu Lake, Xinjiang. *Oceanol Limnol Sin* **24**, 100-108 (1993).
79 Machena, C. Zonation of submerged macrophyte vegetation in Lake Kariba, Zimbabwe and its ecological interpretation. *Vegetatio* **73**, 111-119 (1988).
80 Aladin, N., Filippov, A., Plotnikov, I., Orlova, M. & Williams, W. Changes in the structure and function of biological communities in the Aral Sea, with particular reference to the northern part (Small Aral Sea), 1985--1994: A review. *International Journal of Salt Lake Research* **7**, 301-343 (1998).
81 Gabriel, A. O. & Bodensteiner, L. R. Impacts of riprap on wetland shorelines, upper Winnebago pool lakes, Wisconsin. *Wetlands* **32**, 105-117 (2012).
82 Badzinski, S. S., Ankney, C. D. & Petrie, S. A. in *Limnology and Aquatic Birds* 195-211 (Springer, 2006).
83 Chepinoga, V. V., Bergmeier, E., Rosbakh, S. A. & Fleckenstein, K. M. Classification of aquatic vegetation (Potametea) in Baikal Siberia, Russia, and its diversity in a northern Eurasian context.

Phytocoenologia **43**, 127-167 (2013).

84 Jaikumar, M., Chellaiyan, D., Kanagu, L., Kumar, P. S. & Stella, C. Distribution and succession of aquatic macrophytes in Chilka Lake-India. *Journal of Ecology and the Natural Environment* **3**, 499-508 (2011).

85 Krivonogov, S. K. *et al.* Regional to local environmental changes in southern Western Siberia: evidence from biotic records of mid to late Holocene sediments of Lake Beloye. *Palaeogeography, Palaeoclimatology, Palaeoecology* **331**, 177-193 (2012).

86 Romanova, S. & Kazangapova, N. Theory and practice of selfpurification capacities of natural water in Kazakhstan. *News of the national academy of sciences of the republic of Kazakhstan-series of geology and technical sciences* 41-48 (2018).

87 Villamagna, A. M., Murphy, B. R. & Karpanty, S. M. Community-level waterbird responses to water hyacinth (Eichhornia crassipes). *Invasive Plant Science and Management* **5**, 353-362 (2012).

88 Imentai, A., Thevs, N., Schmidt, S., Nurtazin, S. & Salmurzauli, R. Vegetation, fauna, and biodiversity of the Ile delta and southern Lake Balkhash—A review. *Journal of Great Lakes Research* **41**, 688-696 (2015).

89 Barrientos, C. A. *Fish abundance and community composition in native and non-native littoral aquatic plants at Lake Izabal, Guatemala*, University of Florida, (2005).

90 Tehranchi, M., Shafiei, A. D. & Shaghaghi, S. Studying solutions of development of tourism in Urmia Lake based on SWOT model. *Advances in Environmental Biology*, 4505-4512 (2013).

91 Davies, W. D. Lake Nicaragua fishery resources. *Investigations of the ichthyofauna of Nicaraguan Lakes*, 16 (1976).

92 Cheruiyot, E. *et al.* Evaluating MERIS-based aquatic vegetation mapping in Lake Victoria. *Remote Sensing* **6**, 7762-7782 (2014).

93 Heblinski, J. *et al.* High-resolution satellite remote sensing of littoral vegetation of Lake Sevan (Armenia) as a basis for monitoring and assessment. *Hydrobiologia* **661**, 97-111 (2011).

94 Beklioglu, M., Altinayar, G. & Tan, C. O. Water level control over submerged macrophyte development in five shallow lakes of Mediterranean Turkey. *Archiv für Hydrobiologie* **166**, 535-556 (2006).

95 Ali, M. M., Mageed, A. A. & Heikal, M. Importance of aquatic macrophyte for invertebrate diversity in large subtropical reservoir. *Limnologica-Ecology and Management of Inland Waters* **37**, 155-169 (2007).

96 Green, J. Nilotic lakes of the Western Rift. *The Nile*, 263-286 (2009).